

# Geometric Attitude Control via Contraction on Manifolds with Automatic Gain Selection

Bee Vang<sup>1</sup> and Roberto Tron<sup>2</sup>

**Abstract**—In this paper we propose a new analysis of a simple geometric attitude controller, showing that it is locally exponentially stable and almost globally asymptotically stable; the exponential convergence region is much larger than existing non-hybrid geometric controllers (and covers almost the entire rotation space). The controller’s stability is proved using contraction analysis combined with optimization. The key in this combination is that the contraction metric is a linear matrix inequality with a special structure stemming from the configuration manifold  $SO(3)$ .

As an additional contribution, we propose a general framework to automatically select controller gains by optimizing bounds on the system’s convergence rate; while this principle is quite general, its application is particularly straightforward with our contraction-based analysis.

We demonstrate our results through simulations.

## I. INTRODUCTION

Rigid body attitude control has many useful applications, ranging from aerial robots, to manipulators, camera surveillance systems, and spacecrafts. In particular, the control of a multi-rotor aircraft typically relies on attitude control [1]. For example, to steer a quadrotor, the vehicle must first rotate its body so that it can provide thrust in the desired direction.

Traditional approaches propose controllers based on specific parameterizations of the space of rotations [2]–[4], the most common being Euler angles and quaternions. These controllers, however, cannot offer global convergence guarantees, and often introduce additional complexities and singularities that are due solely to the representation used [2].

On the other hand, geometric controllers [5]–[10] regard the configuration space as a differential manifold (e.g.,  $SO(3)$  for rotations,  $SE(3)$  for rotations and translations,  $SO(3) \times \mathbb{S}^2$  for a rotation plus suspended load, etc.) and use Lyapunov theory (often using a mechanical-energy-like function) to develop an almost globally stable controller with local exponential convergence (for  $SO(3)$ , the typical exponential convergence region is given by a ball of radius  $\frac{\pi}{2}$  around the origin).

The state of the art in terms of attitude controllers is represented by hybrid approaches, such as the one of [11] (which builds upon the work of [12], [13]) or [14]. At a high level, these controllers work by using multiple potential functions inspired by the previous, non-hybrid controllers, but modified and combined in a hybrid fashion so that undesired equilibria or regions of slow convergence are

This work was supported by the National Science Foundation grant NSF CMMI-1728277.

<sup>1</sup>Department of Mechanical Engineering, Boston University, Boston, MA 02215, USA {bvang@bu.edu}

<sup>2</sup>Department of Mechanical and System Engineering, Boston University, Boston, MA 02215, USA {tron@bu.edu}

avoided through switching. As any hybrid controller, these approaches are inherently more complex and computationally more demanding than static controllers due to the logic needed to handle the discrete part of the dynamics.

In most of the papers cited above, the conditions on the control gains to ensure stability are provided, but these are complex to parse (as they typically result from conditions on the eigenvalues of matrices, and might also depend on additional parameters that also need to be specified). Moreover, these works do not provide any method to actually identify suitable coefficients, let alone find a set that is optimal in some sense (e.g., best lower bound on the convergence rate). In all these approaches, it is standard to assume a bound on the maximum angular speed experienced by the rigid body.

Instead of a Lyapunov approach, as in [8], in this paper we will combine contraction analysis with optimization. A recent work that also combines contraction analysis and optimization is [15], where they address the converse problem in  $\mathbb{R}^n$ ; namely, they choose a contraction metric and search (pointwise) for a controller, whereas we choose a (simple) controller, and find a contraction metric (over a large region).

**Paper contributions.** In this paper, we are interested in seeing how far we can push the exponential convergence results for a simple PD, non-hybrid controller (which is the easiest to implement), and provide practitioners with an automatic, principled, and relatively simple way to select valid control gains (for our and other controllers). By using contraction theory, we show that our simple PD controller can have an exponential stability region much larger than previously demonstrated. As a complementary contribution, we propose a general principle to automatically select controller gains that optimize a bound on the convergence rate (using analytical bounds, convex optimization, bisection, and grid search).

## II. PRELIMINARIES AND NOTATION

### A. Riemannian Geometry

We assume some familiarity with Riemannian geometry (see, e.g., [16] for a more in-depth discussion). A rigid body’s attitude in three dimensions can be uniquely represented by a rotation matrix  $R \in SO(3)$ , where  $SO(3) = \{R \in \mathbb{R}^{3 \times 3} : R^T R = I_3, \det(R) = 1\}$ . Let  $\mathfrak{so}(3)$  be the set of all  $3 \times 3$  skew symmetric matrices, then the *tangent space* of  $SO(3)$  at a rotation  $R$  is denoted by  $T_R SO(3) = \{RV : V \in \mathfrak{so}(3)\}$ . A tangent vector  $W \in T_R SO(3)$  can be identified with a

vector  $\omega \in \mathbb{R}^3$  using the hat  $(\cdot)^\wedge$  and vee  $(\cdot)^\vee$  operators:

$$\omega = \begin{bmatrix} \omega_1 \\ \omega_2 \\ \omega_3 \end{bmatrix} \xrightarrow{(\cdot)^\wedge} W = R \begin{bmatrix} 0 & -w_3 & w_2 \\ w_3 & 0 & -w_1 \\ -w_2 & w_1 & 0 \end{bmatrix}. \quad (1)$$

For convenience, we denote the hat operator at the identity  $R = I_3$  as  $\hat{\cdot}$  (i.e., without parentheses). With this notation, the following statements represent the same tangent vector  $W \in T_R SO(3)$ :  $W = (\omega)^\wedge = R\hat{\omega}$ . At a rotation  $R \in SO(3)$ , the *exponential* and *logarithm* maps, which locally transform tangent vectors into points on the corresponding geodesic, and vice versa, are denoted as  $\exp_R : T_R SO(3) \rightarrow SO(3)$  and  $\log_R : U_R \rightarrow T_R SO(3)$ , where  $U_R \subset SO(3)$  is the set around  $R$  for which  $\exp_R$  is diffeomorphic. A metric  $g$  on  $SO(3)$  is a family of inner products  $g : T_R SO(3) \times T_R SO(3) \rightarrow \mathbb{R}$ . The covariant derivative of  $SO(3)$  for any smooth vector fields  $X, Y$  on  $SO(3)$  is denoted as  $\nabla_X Y$ , and provides a way to compute the variation of the field  $Y$  along the flow of  $X$ . Although the choice of the connection is not unique in general, we use the Levi-Civita connection, which is the unique torsion-free connection compatible with the metric  $g$ .

The dynamics of the rigid body evolve on the tangent bundle  $TSO(3) = \{(R, W) : R \in SO(3), W \in T_R SO(3)\}$ , where the state variables are the rotations  $R$  and the angular velocities  $\omega = W^\vee \in \mathbb{R}^3$  [16]. The *tangent space* of  $TSO(3)$  at a point  $(R, W)$  is denoted as  $T_W T_R SO(3)$ . Since  $T_R SO(3)$  is isomorphic to  $\mathbb{R}^3$  through the vee map, its tangent space can be identified with  $T_R SO(3)$  itself. Thus,  $T_W T_R SO(3) = \{(V, U) : V, U \in T_R SO(3)\}$ . We represent tangent vectors in  $T_W T_R SO(3)$  as vertically concatenated matrices, e.g.  $\begin{bmatrix} V \\ U \end{bmatrix}$ .

### B. Rigid Body Dynamics

We model the rigid body rotations by using two reference frames: an inertial frame, and a body-fixed frame with origin at the center of mass. The equations of motion are given by

$$\begin{aligned} \dot{R} &= R\hat{\omega}, \\ \dot{\omega} &= \Gamma - J^{-1}(\omega \times J\omega), \end{aligned} \quad (2)$$

where  $R \in SO(3)$  is the rotation from the body to the inertial frame, while  $\omega \in \mathbb{R}^3$  is the angular velocity,  $J \in \mathbb{R}^{3 \times 3}$  is the inertia matrix, and  $\Gamma \in \mathbb{R}^3$  is the total moment vector (control input), all expressed in the body frame.

### C. Contraction Theory

Next, we briefly review contraction theory (see [17], [18] for details). Contraction analysis was inspired by fluid mechanics, where stability can be viewed as multiple trajectories converging to some nominal motion; in other words, infinitesimal displacements  $\delta_x$  between neighboring trajectories (vector fields, in differential geometry terminology) converge to zero. More precisely, let  $\dot{x} = f(x, t)$  be a nonlinear system evolving on  $\mathbb{R}^n$  (where  $f$  is viewed as a vector field).

We say that the system is contracting if, at any point  $x \in \mathbb{R}^n$ , the infinitesimal displacement between neighboring trajectories vanishes exponentially fast,

$$\|\delta_x(t)\|_M \leq \|\delta_x(0)\|_M e^{-\beta t}. \quad (3)$$

We then have the following result.

*Proposition 1 (Adapted from [17]):* The system  $\dot{x} = f(x, t)$  is contracting if there exist a positive definite matrix  $M$  such that

$$\frac{d}{dt} (\delta_x^T M \delta_x) = \delta_x^T \left( \frac{\partial f^T}{\partial x} M + M \frac{\partial f}{\partial x} \right) \delta_x < -\beta \delta_x^T M \delta_x. \quad (4)$$

In general  $M$  can also be a function of the state  $x$  and time  $t$ ; however, in this paper we only consider constant matrices. More compactly, (3) is equivalent to the matrix inequality

$$\frac{\partial f^T}{\partial x} M + M \frac{\partial f}{\partial x} \leq -\beta M, \quad (5)$$

where  $\beta > 0$  is the minimum guaranteed convergence rate.

These results can be generalized to coordinate-free version for Riemannian manifolds.

*Proposition 2 (Adapted from [18]):* A system  $\dot{x} = f(x, t)$  evolving on a manifold is contracting if there exist a metric  $g$  with Levi-Civita connection  $\nabla$  such that

$$g(\nabla_{\delta_x} f, \delta_x)_M \leq -\beta g(\delta_x, \delta_x)_M \quad (6)$$

for any choice of the vector field  $\delta_x$ .

If the matrix  $M$  represents the coefficients of  $g$  in some local coordinates on the manifold, then (6) reduces to (5).

### III. ATTITUDE CONTROLLER

In this section, we present a geometric attitude controller, and develop a framework to study the closed-loop system's stability. Without loss of generality, we stabilize to the point on the tangent bundle where  $R_d = I_3$  and  $\omega_d = [0, 0, 0]^T$ . First, we choose a cost (or potential) function  $\Psi(R, R_d)$  which is star-convex [19] with respect to  $R_d$  in the neighborhood  $U_{R_d}$ , bounded, and such that  $\Psi(R_d, R_d) = 0$ ; for instance, in this paper we naturally choose

$$\Psi(R, R_d) = \frac{1}{2} d(R, R_d)^2 = \frac{1}{2} \|(\log_R R_d)^\vee\|^2, \quad (7)$$

which is the squared geodesic distance on  $SO(3)$  with metric

$$g(R\hat{\alpha}, R\hat{\xi}) = \frac{1}{2} \text{tr}(\hat{\alpha}^T \hat{\xi}). \quad (8)$$

We define the rotation and velocity errors as

$$e_R = (\text{grad}(\Psi))^\vee, \quad (9)$$

$$e_\omega = \omega - \omega_d = \omega, \quad (10)$$

where  $\text{grad}(\cdot)$  is the gradient operator. We then arrive to an attitude controller of the classical PD form

$$\Gamma_R = J^{-1}(\omega \times J\omega) - k_d e_R - k_v e_\omega, \quad (11)$$

where the feedforward term cancels the gyroscopic effects, and  $k_d, k_v$  are positive feedback gains. The closed-loop system equations using controller (11) become

$$\begin{aligned} \dot{R} &= R\hat{\omega} \doteq f_R(R, \omega), \\ \dot{\omega} &= -k_d e_R - k_v e_\omega \doteq f_\omega(R, \omega), \end{aligned} \quad (12)$$

where the system dynamics evolve on the tangent bundle.

We study the stability of (12) through optimization by following four steps:

- 1) Derive the generalized contraction metric (6) for the closed-loop system;

- 2) Diagonalize and bound the contraction metric to obtain linear objectives and constraints;
- 3) Solve for the matrix  $M$  through optimization such that (6) is satisfied for given  $k_d, k_v, \beta$ ;
- 4) Automatically select gains  $k_d, k_v$  while maximizing  $\beta$  through a grid-bisection search.

1) *Closed-Loop System and Contraction*: The system  $(f_R, f_\omega)$  defines a vector field on the tangent bundle  $TSO(3)$ . To apply (6), we have to first define the covariant derivative on the tangent bundle. In general, finding a closed-form expression for the covariant derivative is difficult; however, it is available for  $SO(3)$  [20]. In addition, based on the work of [21] and [22], the covariant derivative and metric on  $SO(3)$  can be used to induce their counterparts on the tangent bundle  $TSO(3)$ ; we use (8) as our base metric and define an induced metric  $\tilde{g}$  on  $TSO(3)$  as

$$\tilde{g}\left(\begin{bmatrix} R\hat{\zeta} \\ R\hat{\alpha} \\ R\hat{\eta} \end{bmatrix}, \begin{bmatrix} R\hat{\zeta} \\ R\hat{\alpha} \\ R\hat{\eta} \end{bmatrix}\right) = \frac{1}{2} \text{tr}\left(\begin{bmatrix} \hat{\zeta} \\ \hat{\eta} \end{bmatrix}^T (M \otimes I_3) \begin{bmatrix} \hat{\alpha} \\ \hat{\xi} \end{bmatrix}\right) \quad (13)$$

where  $R \in SO(3)$ ,  $\alpha, \xi, \eta, \zeta \in \mathbb{R}^3$  represent tangent vectors,

$$M = \begin{bmatrix} m_1 & m_2 \\ m_2 & m_3 \end{bmatrix}, \quad (14)$$

and  $\otimes$  is the Kronecker product. The induced metric  $\tilde{g}$  is a metric on  $TSO(3)$  if  $M$  is positive definite, and a closed form expression for the covariant derivative  $\tilde{\nabla}$  can be found (see [23] for a detailed derivation). Using  $\tilde{\nabla}$ , and letting  $\delta_x = \begin{bmatrix} R\hat{\zeta} \\ R\hat{\eta} \end{bmatrix}$  for  $\zeta, \eta \in \mathbb{R}^3$ , the contraction condition (6) for the closed-loop system (12) becomes

$$\begin{bmatrix} \zeta \\ \eta \end{bmatrix}^T \mathcal{M} \begin{bmatrix} \zeta \\ \eta \end{bmatrix} \leq 0 \quad (15)$$

where  $\mathcal{M}$  is composed of four block matrices given below:

$$\mathcal{M}_{1,1} = \frac{m_2}{4} \hat{\omega}^2 - m_2 k_d De_R + m_1 \beta I_3, \quad (16)$$

$$\begin{aligned} \mathcal{M}_{2,1} = & \frac{m_3 k_v - m_2}{4} \hat{\omega} + \frac{m_3}{8} \hat{\omega}^2 + \frac{m_3 k_d}{4} \hat{e}_R \\ & - \frac{m_3 k_d}{2} De_R + \left( \beta m_2 + \frac{m_1 - m_2 k_v}{2} \right) I_3, \end{aligned} \quad (17)$$

$$\mathcal{M}_{1,2} = \mathcal{M}_{2,1}^T, \quad (18)$$

$$\mathcal{M}_{2,2} = (m_3 \beta + m_2 - m_3 k_v) I_3, \quad (19)$$

and  $De_R$  is the differential of the rotation error (9).

If the matrix  $\mathcal{M}$  is negative semidefinite, then (15) (and (6)) is satisfied. By contraction analysis, the closed-loop system is exponentially converging at the current state with a minimum rate of  $\beta$ . However, this condition needs to be satisfied for all states  $R$  in a neighborhood  $U_{R_d}$  of  $R_d$  and  $\omega \in \mathbb{R}^3$  in order to guarantee local convergence. The challenge now is to choose parameters  $m_1, m_2, m_3$  for given parameters  $k_d, k_v, \beta$  such that  $\mathcal{M} \leq 0$  for all states in the neighborhood of  $R_d$ .

2) *Matrix Decomposition*: We pose the problem of finding  $m_1, m_2, m_3$  satisfying (15) given  $k_d, k_v, \beta$  as a semidefinite programming problem. Minimizing the LHS of (15) is equivalent to minimizing the maximum eigenvalue of  $\mathcal{M}$ . Unfortunately, we have to consider (15) for all possible  $(R, \omega)$ , resulting in an infinite number of constraints. However, although the analytical equations for all eigenvalues of  $\mathcal{M}$

are non-convex with respect to  $m_1, m_2, m_3$ , the elements of  $\mathcal{M}$  are all linear in the same variables. We therefore propose the following strategy:

- 1) decompose the matrix  $\mathcal{M}$  in two matrices, one dependent on  $R$  and one dependent on  $\omega$ ,
- 2) perform a state-dependent similarity transformation such that (15) does not depend directly on  $(R, \omega)$  but on the eigenvalues of  $De_R$ , and the maximum norm of  $\omega$ , and
- 3) relax the constraints using Gershgorin discs so that (15) can be bounded by linear constraints.

In the first step, we take the symmetric part of the matrix  $\mathcal{M}$  and decompose it as the sum of two symmetric matrices  $\Omega, P$ . The matrix  $\Omega$  is composed of four blocks:

$$\Omega_{1,1} = \frac{m_2}{4} \hat{\omega}^2, \quad (20)$$

$$\Omega_{2,1} = \frac{m_3 k_v - m_2}{4} \hat{\omega} + \frac{m_3}{8} \hat{\omega}^2, \quad (21)$$

$$\Omega_{1,2} = \Omega_{2,1}^T, \quad (22)$$

$$\Omega_{2,2} = 0_3. \quad (23)$$

The  $P$  matrix is also composed of four blocks:

$$P_{1,1} = -\frac{m_2 k_d}{2} (De_R + De_R^T) + m_1 \beta I_3, \quad (24)$$

$$P_{2,1} = \frac{m_3 k_d}{4} \hat{e}_R - \frac{m_3 k_d}{2} De_R + \left( \beta m_2 + \frac{m_1 - m_2 k_v}{2} \right) I_3, \quad (25)$$

$$P_{1,2} = P_{2,1}^T, \quad (26)$$

$$P_{2,2} = \mathcal{M}_{2,2} = (m_3 \beta + m_2 - m_3 k_v) I_3. \quad (27)$$

The motivation for this decomposition is that the matrices may be independently diagonalized, which allows us to remove the explicit dependency on  $(R, \omega)$  while extracting bounds on the eigenvalues. Since  $\hat{\omega}$  and  $\hat{\omega}^2$  share the same eigenvectors, the matrix  $\Omega$  can be diagonalized as

$$\Omega = T_\Omega^{-1} \Omega_D T_\Omega; \quad (28)$$

where  $\Omega_D$  contains four diagonal blocks:

$$\Omega_{D1,1} = \frac{m_2}{4} \|\omega\|^2 \begin{bmatrix} 0 & 0 & 0 \\ 0 & -1 & 0 \\ 0 & 0 & -1 \end{bmatrix}, \quad (29)$$

$$\Omega_{D2,1} = \frac{m_3}{8} \|\omega\|^2 \begin{bmatrix} 0 & 0 & 0 \\ 0 & -1 & 0 \\ 0 & 0 & -1 \end{bmatrix} + \alpha \begin{bmatrix} 0 & 0 & 0 \\ 0 & i & 0 \\ 0 & 0 & -i \end{bmatrix}, \quad (30)$$

$$\Omega_{D1,2} = \overline{\Omega_{D2,1}}, \quad (31)$$

$$\Omega_{D2,2} = 0_3, \quad (32)$$

with the transformation matrix

$$T_\Omega = \begin{bmatrix} V_\omega & 0_3 \\ 0_3 & V_\omega \end{bmatrix}, \quad (33)$$

such that  $V_\omega$  is the similarity transformation matrix that diagonalizes  $\hat{\omega}$ ,  $i = \sqrt{-1}$  is the unit imaginary number, and

$$\alpha = \|\omega\| \frac{m_3 k_v - m_2}{4}. \quad (34)$$

*Remark 1*: The eigenvalues (and Gershgorin discs) of  $\Omega$  scale with  $\|\omega\|$ . It might not be possible to find parameters

$m_1, m_2, m_3$  such that  $\mathcal{M} \leq 0$  for all possible  $\omega \in \mathbb{R}^3$ . Therefore, as it is standard in the literature, we assume that there is a bound on the maximum speed  $\|\omega\|_{\max}$ .

We can perform a similar decomposition for the matrix  $P$ , with the difference that the two matrices  $\hat{e}_R$  and  $De_R$ , in general, might not have the same eigenvectors. Nonetheless, we can arrive at the decomposition

$$P = T_P^{-1} P_D T_P \quad (35)$$

where  $P_D$  is composed of four block matrices as follows:

$$P_{D1,1} = -\frac{m_2 k_d}{2} (\Lambda + \Lambda^T) + m_1 \beta I_3, \quad (36)$$

$$P_{D2,1} = -\frac{m_3 k_d}{2} \Lambda + \frac{2\beta m_2 + m_1 - m_2 k_v}{2} I_3 + \frac{m_3 k_d}{4} e_{RP}, \quad (37)$$

$$P_{D1,2} = \overline{P_{D2,1}}, \quad (38)$$

$$P_{D2,2} = (m_3 \beta + m_2 - m_3 k_v) I_3, \quad (39)$$

where  $e_{RP} = V_P^{-1} \hat{e}_R V_P$ , with the transformation matrix

$$T_P = \begin{bmatrix} V_P & 0_3 \\ 0_3 & V_P \end{bmatrix}, \quad (40)$$

such that  $V_P$  is the similarity transformation matrix that diagonalizes  $De_R$ , and  $\Lambda$  is the diagonal matrix containing the eigenvalues of  $De_R$ .

Since similar matrices have the same eigenvalues, we focus on constraining  $\Omega_D$  and  $P_D$ , which in turn constrain the original  $\mathcal{M}$  matrix. The transformation matrices  $T_\Omega$  and  $T_P$  have been chosen such that many of the off-diagonal elements of  $\Omega_D$  and  $P_D$  are zero. This fact is useful for obtaining possibly tighter bounds on the Gershgorin discs since the radii will be composed of fewer absolute value terms. Up to this point, the derivations do not depend on the choice of the cost  $\Psi$ ; we later show that for our choice of cost function (7), the dependency of the constraints will be limited to the *minimum and maximum values* of the eigenvalues of  $De_R$  and  $\|\omega\|$ , which can be, respectively, either precomputed or known; as a result, the constraints on  $\mathcal{M}$  will only depend on  $m_1, m_2, m_3$ .

3) *Optimization Problem*: Now that we have exploited the structure of the matrix  $\mathcal{M}$ , we use it to formulate an optimization problem using Gershgorin discs (see [24]). First, recall that, by the interlacing theorem,

$$\lambda_{\max}(A + B) \leq \lambda_{\max}(A) + \lambda_{\max}(B) \quad (41)$$

which implies

$$\lambda_{\max}(A + B) \leq \mathcal{D}_{\max}(A) + \mathcal{D}_{\max}(B) \quad (42)$$

where  $\lambda_{\max}$  is the largest eigenvalue and  $\mathcal{D}_{\max}$  is the largest real number encompassed by any Gershgorin discs. The inequality (42) effectively allows us to relax the constraints for  $\mathcal{M}$  in two parts, some for  $\Omega_D$  and some for  $P_D$ . Using this fact, we propose the feasibility problem in Proposition 3 below to find suitable parameters  $m_1, m_2, m_3$ . The goal of the feasibility problem is to push the Gershgorin discs of  $\Omega_D$  and  $P_D$  as far towards negative infinity as possible. The idea being that we want the sum  $\mathcal{D}_{\max}(\Omega_D) + \mathcal{D}_{\max}(P_D) \leq 0$ , so that  $\lambda_{\max}(\mathcal{M}) \leq 0$ , thus satisfying (15).

*Proposition 3:* The system given in (2) with the controller in (11) is locally exponentially stable with minimum convergence rate  $\beta > 0$  for all  $R$  in a neighborhood  $U_{R_d}$  of  $R_d$  and  $\|\omega\| \leq \|\omega\|_{\max} < 4$ , if there exist  $m_1, m_2, m_3 > 0$  satisfying

$$\mathcal{D}_{\max}(P_D) + \frac{m_3}{8} \|\omega\|_{\max}^2 + \|\omega\|_{\max} \frac{m_3 k_v - m_2}{4} \leq 0 \quad (43)$$

$$\begin{bmatrix} m_1 & m_2 \\ m_2 & m_3 \end{bmatrix} > 0 \quad (44)$$

$$P_{Di,i} \leq 0, \quad i = \{1, \dots, 6\} \quad (45)$$

for given  $k_d, k_v, \beta, \|\omega\|_{\max}$ , and all  $R \in U_{R_d}$ .

Note that (44) is necessary to validate the metric on the tangent bundle.

*Proof:* The objective is to find  $m_1, m_2, m_3$  such that  $\mathcal{D}_{\max}(P_D) + \mathcal{D}_{\max}(\Omega_D) \leq 0$  is true for all  $R \in U_{R_d}$  and  $\|\omega\| \leq \|\omega\|_{\max}$ . By inspection of the  $\Omega_D$  matrix (29)-(32), there are three unique Gershgorin discs bounding the eigenvalues given below,

$$\mathcal{D}_{\Omega_D 1} = 0, \quad (46)$$

$$\mathcal{D}_{\Omega_D 2} = -\frac{m_2}{4} \|\omega\|^2 + \left| \alpha i - \frac{m_3}{8} \|\omega\|^2 \right|, \quad (47)$$

$$\mathcal{D}_{\Omega_D 3} = \left| \alpha i - \frac{m_3}{8} \|\omega\|^2 \right|, \quad (48)$$

where  $\alpha$  is defined in (34). The discs above state that  $\mathcal{D}_{\max}(\Omega_D) \geq 0$ , therefore  $\mathcal{D}_{\max}(P_D) \leq 0$ . To achieve  $\mathcal{D}_{\max}(P_D) \leq 0$ , the centroids of the  $P_D$  matrix must be nonpositive, thus the constraint (45) is necessary. Together, constraints (44) and (45) imply that  $m_1, m_2, m_3 > 0$ .

Next,  $\mathcal{D}_{\Omega_D 3}$  is the maximum bound on the eigenvalues of  $\Omega_D$  since it is always greater than or equal to zero, and is greater than or equal to  $\mathcal{D}_{\Omega_D 2}$  due to the negative term. Furthermore,  $\mathcal{D}_{\Omega_D 3}$  can be bounded from above as follows

$$\begin{aligned} \mathcal{D}_{\Omega_D 3} &= \sqrt{\left( \frac{m_3}{8} \|\omega\|^2 \right)^2 + \left( \|\omega\| \frac{m_3 k_v - m_2}{4} \right)^2} \\ &\leq \frac{m_3}{8} \|\omega\|^2 + \|\omega\| \frac{m_3 k_v - m_2}{4}. \end{aligned} \quad (49)$$

The second line is obtained in two steps: 1) relaxing the first line using the *subadditive* property of the square root function [25], and 2) by observing that the centroids of  $P_{D2,2} \leq 0$ , thus  $m_3 k_v \geq m_2$  and the absolute value sign can be dropped. Then letting

$$\mathcal{D}_{\max}(\Omega_D) = \frac{m_3}{8} \|\omega\|^2 + \|\omega\| \frac{m_3 k_v - m_2}{4}, \quad (50)$$

$\mathcal{D}_{\max}(\Omega_D)$  is maximized when  $\|\omega\| = \|\omega\|_{\max}$  since this is a quadratic function in  $\|\omega\|$  with positive coefficients. In addition, if  $\|\omega\|_{\max} \geq 4$ , then the problem is infeasible since the maximum bound on the Gershgorin discs centered at  $P_{D2,2}$  summed with  $\mathcal{D}_{\max}(\Omega_D)$  is always greater than zero. However, this limitation can be removed by relaxing (50) (as discussed in Remark 2 below).

Finally if the problem is feasible for given  $k_d, k_v, \beta, \|\omega\|_{\max} < 4$ , and all  $R \in U_{R_d}$ , then

$$\begin{aligned} 0 &\geq \mathcal{D}_{\max}(P_D) + \frac{m_3}{8} \|\omega\|_{\max}^2 + \|\omega\|_{\max} \frac{m_3 k_v - m_2}{4} \\ &\geq \lambda_{\max}(P_D) + \lambda_{\max}(\Omega_D) \geq \lambda_{\max}(\mathcal{M}), \end{aligned} \quad (51)$$

and, by contraction theory, the system is locally exponentially stable for all  $R \in U_{R_d}$ ,  $\|\omega\| \leq \|\omega\|_{\max}$ , and with minimum convergence rate  $\beta$ .  $\blacksquare$

*Remark 2:* The constraint  $\|\omega\|_{\max} < 4$  is not an intrinsic limitation of the system. Instead, it is a consequence of the relaxations used to obtain (50). If the application requires  $\|\omega\|_{\max} \geq 4$ , equation (50) can be relaxed in the following way, with  $p, q \in \mathbb{R}_{>0}$ ,

$$\mathcal{D}_{\max}(\Omega_D) \leq q \frac{m_3}{8} \|\omega\|_{\max}^2 + \frac{1}{p} \|\omega\|_{\max} \frac{m_3 k_v - m_2}{4}, \quad (52)$$

where  $p \geq 1$  is chosen such that  $\|\omega\|_{\max} < 4p$  and

$$\begin{aligned} q &= \frac{2}{\|\omega\|_{\max}} \left(1 - \frac{1}{p}\right) k_v + 1 \\ &\geq \frac{2}{\|\omega\|_{\max}} \left(1 - \frac{1}{p}\right) \left(k_v - \frac{m_2}{m_3}\right) + 1. \end{aligned} \quad (53)$$

The second line is the  $q$  required to achieve equality in (52), which can be relaxed to the value in the first line (where all parameters are known), because  $m_2, m_3 > 0$ . For simplicity, in this paper we simply assume  $\|\omega\|_{\max} < 4$  and  $p = q = 1$ . Notwithstanding, we show in the simulations of Section IV that the controller remains stable for  $\|\omega\| \gg 4$ .

*Remark 3:* Since (15) is homogeneous in  $M$ , if a particular solution  $M^*$  is found, then any scaling of  $M^*$  will also give a valid solution. Therefore, to improve the numerical stability of the solver, we add the constraint  $m_1 = 1$ .

*Remark 4:* In general,  $\mathcal{D}_{\max}(P_D)$  depends on  $R \in SO(3)$  and the eigenvalues of the differential  $D e_R$ , resulting in a potentially infinite number of constraints for the Gershgorin discs. In our case, using the fact that the cost function (7) is symmetric with respect to the identity, we can bound the eigenvalues, for any  $R$ , using  $\|\omega\|_{\max}$  alone.

The next step is to determine when Proposition 3 is feasible for our cost function (7). To begin, the gradient of  $\Psi$  is given by [26, Prop. 2.2.1] as

$$\text{grad}(\Psi) = -\log_R I_3 = R \log_{I_3} R. \quad (54)$$

Since the eigenvectors of  $\log_{I_3} R$  and its differential  $D(\log_{I_3} R)$  are the same [26], all block matrices of the  $P$  matrix (35) can be simultaneously diagonalized by choosing  $V_P$  to be the matrix that diagonalizes  $\log_{I_3} R$ . The resulting  $P_D$  matrix is given by:

$$P_{D1,1} = -m_2 k_d \text{Re}(\Lambda) + m_1 \beta I_3, \quad (55)$$

$$P_{D2,1} = -\frac{m_3 k_d}{2} \text{Re}(\Lambda) + \left(m_2 \beta + \frac{m_1 - m_2 k_v}{2}\right) I_3, \quad (56)$$

$$P_{D1,2} = P_{D2,1}, \quad (57)$$

$$P_{D2,2} = (m_3 \beta + m_2 - m_3 k_v) I_3, \quad (58)$$

where

$$e_{RP} = \begin{bmatrix} 0 & 0 & 0 \\ 0 & \theta i & 0 \\ 0 & 0 & -\theta i \end{bmatrix}, \quad (59)$$

the diagonal matrix  $\Lambda$  is given in [26, Prop. E.2.1]

$$\Lambda = \begin{bmatrix} 1 & 0 & 0 \\ 0 & \frac{\theta}{2} \cot \frac{\theta}{2} + \frac{\theta}{2} i & 0 \\ 0 & 0 & \frac{\theta}{2} \cot \frac{\theta}{2} - \frac{\theta}{2} i \end{bmatrix}, \quad (60)$$

$\cot$  is the cotangent function,  $\text{Re}(\cdot)$  is the real part of a complex matrix, and

$$\theta = \left\| (\log_{I_3} R)^\vee \right\|. \quad (61)$$

The  $\theta$  parameter represents the geodesic distance between any two rotations on  $SO(3)$  with respect to the metric (8), and is bounded between 0 and  $\pi$  [26]. Thus, the real part of the eigenvalue  $\frac{\theta}{2} \cot \frac{\theta}{2} \in (0, 1)$  is continuous for  $\theta \in [\pi, 0]$ . Since  $\theta$  is symmetric, the  $P_D$  matrix can be parameterized by some fixed  $\theta_{\max} < \pi$ , instead of  $R$ , which covers all  $R$  within  $\theta_{\max}$  distance of  $I_3$ .

By inspection, there are four unique Gershgorin discs bounding the eigenvalues of the  $P_D$  matrix above:

$$\mathcal{D}_{P_D1} = -m_2 k_d + m_1 \beta + \left| -\frac{m_3 k_d}{2} + \gamma \right| \quad (62)$$

$$\mathcal{D}_{P_D2} = -m_2 k_d \Theta + m_1 \beta + \left| -\frac{m_3 k_d}{2} \Theta + \gamma \right| \quad (63)$$

$$\mathcal{D}_{P_D3} = m_3 \beta + m_2 - m_3 k_v + \left| -\frac{m_3 k_d}{2} + \gamma \right| \quad (64)$$

$$\mathcal{D}_{P_D4} = m_3 \beta + m_2 - m_3 k_v + \left| -\frac{m_3 k_d}{2} \Theta + \gamma \right|, \quad (65)$$

where

$$\gamma = m_2 \beta + \frac{m_1 - m_2 k_v}{2}, \quad \Theta = \frac{\theta}{2} \cot \frac{\theta}{2}. \quad (66)$$

The maximum bound on the  $P_D$  matrix can be summed with (50) and used as the objective function of an optimization problem to find suitable  $m_1, m_2, m_3$  that satisfies Proposition 3. The optimization problem is posed in Proposition 4.

*Proposition 4:* The system in (2) with controller (11), cost function (7), and given parameters  $k_d, k_v, \beta > 0$ ,  $0 \leq \|\omega\|_{\max} < 4$ , and  $0 < \theta_{\max} < \pi$  is locally exponentially stable with minimum convergence rate  $\beta$  for all  $R$  within  $\theta_{\max}$  distance of  $I_3$  and  $\|\omega\| \leq \|\omega\|_{\max}$  if the optimization problem:

$$\begin{aligned} &\underset{m_1, m_2, m_3}{\text{minimize}} \quad \max(\mathcal{N}) + \mathcal{D}_{\max}(\Omega_D) \\ &\text{subject to} \quad \begin{bmatrix} m_1 & m_2 \\ m_2 & m_3 \end{bmatrix} > 0 \\ &\quad P_{Di,i} \leq 0 \quad i = \{1, \dots, 6\} \end{aligned} \quad (67)$$

where  $\mathcal{D}_{\max}(\Omega_D)$  is defined in (50) and

$$\mathcal{N} = \{\mathcal{D}_{P_D1}, \mathcal{D}_{P_D2}, \mathcal{D}_{P_D3}, \mathcal{D}_{P_D4}\}, \quad (68)$$

is feasible such that:  $\max(\mathcal{N}) + \mathcal{D}_{\max}(\Omega_D) \leq 0$ .

*Proof:* The proof follows directly from Proposition 3.  $\blacksquare$

*Remark 5:* Note that as  $\theta \rightarrow 0, \Theta \rightarrow 1$ , then (63) and (65) are redundant. Therefore, we only have to consider the case when  $\theta = \theta_{\max}$ .

*4) Automated Gain Selection:* In Section III-3, an optimization (more precisely, feasibility) problem was proposed to find parameters  $m_1, m_2, m_3$  such that the contraction matrix  $\mathcal{M} \leq 0$  for given  $k_d, k_v, \beta, \|\omega\|_{\max}$ , and  $\theta_{\max}$ . However, the optimization problem might be infeasible for the given parameters, and even if it is feasible, it might not provide the best convergence guarantees. In this section, we introduce a grid-bisection search algorithm to automatically select the

best gains  $k_d, k_v$  with the largest minimum convergence rate  $\beta$  for given  $\|\omega\|_{\max}$  and  $\theta_{\max}$ . The algorithm is given in Algorithm 1 where  $\beta$  is bounded between 0 and  $\beta_{\max} > 0$ .

**Algorithm 1** Grid-bisection search algorithm to find  $k_d, k_v$  with largest minimum convergence rate  $\beta$  that satisfies Proposition 4. The system input parameters are the maximum angular speed  $\|\omega\|_{\max}$ , maximum distance error  $\theta_{\max}$ , list of rotation error gains  $k_dList$ , list of angular velocity error gains  $k_vList$ , and maximum convergence rate bound  $\beta_{\max}$ .

---

**Require:**  $k_dList, k_vList, \|\omega\|_{\max}, \theta_{\max}, \beta_{\max}$

```

for  $k_d = k_dList$  do
  for  $k_v = k_vList$  do
     $\beta', m'_i = \text{bisectionSearch}(k_d, k_v, \|\omega\|_{\max}, \theta_{\max})$ 
    {Solve optimization problem in Proposition 4}
     $grid \leftarrow k_d, k_v, \beta', m'_i$ 
  end for
end for
return  $k_d^*, k_v^*, \beta^*, m_i^* = \text{findMaxBeta}(grid)$ 
```

---

*Remark 6:* The algorithm can be improved by skipping the bisection search for any combination of  $k_d$  and  $k_v$  that does not meet the requirements of Theorem 1.

The goal of Algorithm 1 is to solve the following problem. Given a set of possible rotation error gains  $k_dList$  and angular velocity error gains  $k_vList$ , a maximum angular speed  $\|\omega\|_{\max}$ , and a maximum distance error  $\theta_{\max}$ , find the combination of gains that produces the largest  $\beta$  satisfying Proposition 4. To solve this, the algorithm first pairs each rotation error gain with each angular velocity error gain. Then for each combination, it maximizes the convergence rate using a bisection search with upper and lower bounds defined by  $\beta_{\max}$  and 0, respectively. Within the bisection search, the algorithm solves the optimization problem in Proposition 4 using the assigned gains and system parameters. Finally, the algorithm selects the combination of gains with the largest rate  $\beta$ .

*Remark 7:* In principle, a similar strategy could be used to select gains for any controller for which an explicit bound on the convergence rate can be computed (such as, for instance, the one from [8]). However, our results based on convex optimization greatly simplify the implementation.

Next, for given  $k_d, \beta, \|\omega\|_{\max}$ , and  $\theta_{\max}$ , we wish to better characterize the set of  $k_v$ 's such that the optimization problem may be feasible. The results are stated in the theorem below.

*Theorem 1:* Given any  $k_d, \beta > 0$ ,  $0 \leq \|\omega\|_{\max} < 4$ , and  $0 < \theta_{\max} < \pi$ , then a necessary condition for Proposition 4 to be satisfied is

$$k_v \geq -\frac{(k_d\Theta_{\max} + 1)(\|\omega\|_{\max}^2 + 2k_d - 2k_d\Theta_{\max})}{2k_d\Theta_{\max}(\|\omega\|_{\max} - 4)}, \quad (69)$$

where

$$\Theta_{\max} = \frac{\theta_{\max}}{2} \cot \frac{\theta_{\max}}{2} \in (0, 1). \quad (70)$$

*Proof:* Parts of the proof are omitted due to page limit.

The requirement  $\max(\mathcal{N}) + \mathcal{D}_{\max}(\Omega_D) \leq 0$  represents eight constraints. To find the limiting  $k_v$ , let  $\beta = 0$ . By inspection

and permutations, we found that the four limiting (basic) constraints are

$$\begin{aligned} m_2 \left( -k_d\Theta_{\max} - \frac{k_v}{2} - \frac{\|\omega\|_{\max}}{4} \right) + \frac{1}{2} \\ m_3 \left( -\frac{k_d\Theta_{\max}}{2} + \frac{\|\omega\|_{\max}^2}{8} + \frac{k_v\|\omega\|_{\max}}{4} \right) \leq 0 \end{aligned} \quad (71)$$

$$\begin{aligned} m_2 \left( 1 - \frac{k_v}{2} - \frac{\|\omega\|_{\max}}{4} \right) + \frac{1}{2} \\ m_3 \left( -k_v - \frac{k_d\Theta_{\max}}{2} + \frac{\|\omega\|_{\max}^2}{8} + \frac{k_v\|\omega\|_{\max}}{4} \right) \leq 0 \end{aligned} \quad (72)$$

$$\begin{aligned} m_2 \left( 1 + \frac{k_v}{2} - \frac{\|\omega\|_{\max}}{4} \right) - \frac{1}{2} \\ m_3 \left( -k_v + \frac{k_d}{2} + \frac{\|\omega\|_{\max}^2}{8} + \frac{k_v\|\omega\|_{\max}}{4} \right) \leq 0 \end{aligned} \quad (73)$$

$$m_3 > m_2^2 \quad (74)$$

where we have set  $m_1 = 1$  (see Remark 3). Each one of the first three constraints bounds a half-plane in  $m_2, m_3$  for any fixed  $k_v$ . If there is an overlapping region such that  $m_3 > m_2^2$ , then the constraints are satisfied. Consider the worst case when the boundary of the first three constraints meet at a point. In other words when equations (71), (72), and (73) all equal zero. Solving this system of equations for  $m_2, m_3$ , and  $k_v$  yields

$$k_v = -\frac{(k_d\Theta_{\max} + 1)(\|\omega\|_{\max}^2 + 2k_d - 2k_d\Theta_{\max})}{2k_d\Theta_{\max}(\|\omega\|_{\max} - 4)} \quad (75)$$

$$m_2 = \frac{2k_d\Theta_{\max}(\|\omega\|_{\max} - 4)(\|\omega\|_{\max}^2 + 2k_d - 2k_d\Theta_{\max})}{-\mathcal{A}} \quad (76)$$

$$m_3 = \frac{4k_d^2\Theta_{\max}^2(\|\omega\|_{\max} - 4)^2}{\mathcal{A}} \quad (77)$$

where

$$\begin{aligned} \mathcal{A} = k_d^3\Theta_{\max}[\Theta_{\max}^2(2\|\omega\|_{\max}^2 - 16\|\omega\|_{\max} + 36) \\ + \Theta_{\max}(2\|\omega\|_{\max}^2 - 16\|\omega\|_{\max} + 24) + 4] \\ + k_d^2[\Theta_{\max}^2(4 - 4\|\omega\|_{\max}^2) + \Theta_{\max}(4\|\omega\|_{\max}^2 - 8) + 4] \\ + k_d\|\omega\|_{\max}^2[\Theta_{\max}(\|\omega\|_{\max}^2 - 4) + 4] + \|\omega\|_{\max}^4. \end{aligned} \quad (78)$$

It is straightforward to show that  $m_3 - m_2^2 > 0$  and that  $m_2, m_3, k_v > 0$  under the assumptions on the given parameters. This result indicates that there is always a feasible solution for the constraints given sufficiently high  $k_v$  and  $\beta = 0$ . To validate that (71)-(74) are indeed the limiting (non-redundant) constraints, we back substitute the solutions into the original eight constraints, and verify that they are all satisfied.

Next, we show that for  $\beta > 0$ ,  $k_v$  must be greater than or equal to the value in (75). By performing the same analysis as before, we obtain new solutions for  $m_2, m_3$ , and  $k_v$  that depends on  $\beta$ . It can be shown, by inspection, that the new  $k_v$  obtained in this way must be greater than or equal to (75). ■

*Remark 8:* In general, the four limiting constraints (71)-(74) may not be the limiting constraints for all  $\beta > 0$ .

However, if the optimization problem is not feasible for  $\beta = 0$  or  $\beta > 0$  but small, then it cannot be feasible for any arbitrary  $\beta > 0$ .

*Remark 9:* Note that  $\theta_{\max} = \pi$  causes the  $\text{Re}(\Lambda)$  matrix to become singular, rendering the problem infeasible, hence we cannot achieve global exponential stability, as expected [27]. However, for any angle  $\theta_{\max} < \pi$ , (69) provides a value of  $k_v$  that guarantees exponential convergence in the set of rotations within  $\theta_{\max}$  distance of  $R_d$ . Therefore, this simple PD controller can achieve quasi-global exponential stability, which is much larger than what was reported in previous results in the literature.

*Remark 10:* Simple almost-global asymptotic convergence can be proven by using Lyapunov theory with the energy-like function  $V(R, \omega) = \Psi(R, R_d) + \frac{1}{k_d} \|\omega\|^2$  (see, e.g., [5]).

#### IV. RESULTS AND SIMULATION

In this section, we validate the controller and theory presented in Section III with a simulation. Recall that we are stabilizing to the point  $R_d = I_3$  and  $\omega_d = [0, 0, 0]^T$ . The system and Algorithm 1 parameters are reproduced in Table I, and the initial attitude  $R_0$  has been randomly selected to be  $\theta_{\max}$  distance away from the identity  $I_3$ . The algorithm results are shown in Table II where we solved the optimization problem in Proposition 4 as a semidefinite program using the CVX modeling system and SDPT3 solver [28]. The algorithm selected the best  $k_d, k_v$  such that suitable  $m_1, m_2, m_3$  are found to guarantee minimum convergence rate  $\beta = 0.0292$ , although the actual rate is in fact much faster (see Figure 2). The looseness of the bound could be due to several reasons, such as the splitting of the  $\mathcal{M}$  matrix into the  $\Omega$  and  $P$  matrices, the use of the Gershgorin discs, and the fact that the bound needs to hold in a large convergence basin (large  $\theta_{\max}$ ). Note that we have utilized Remark 3 and constrained  $m_1 = 1.000$  for the optimization problem. The optimal  $\beta$  for each pair of  $k_d$  and  $k_v$  gains are shown in Figure 1. As predicated by Theorem 1, for any particular  $k_d$  there is a minimum  $k_v$  such that a nonzero  $\beta$  can be found to satisfy Proposition 4.

To confirm the results of our algorithm, we simulate the closed-loop dynamics in Matlab R2018b using 'ode45' and verify that the contraction metric (15) holds throughout the trajectory. The simulation results with the tracking errors are shown in Fig. 2. From the first two plots, it can be concluded that the system with angular speed much greater than  $\|\omega\|_{\max} = 2$  converges, seemingly with an exponential rate.

TABLE I: System and Algorithm 1 Parameters

Parameter	Value	Description
$J$	$\text{diag}(5,2,1)$	Diagonal matrix with values 5,2,1
$k_d$ List	$[0.1:1.0091:100]$	Array from 0.1 to 100, stepsize 1.0091
$k_v$ List	$[0.1:1.0091:100]$	Array from 0.1 to 100, stepsize 1.0091
$\ \omega\ _{\max}$	2	Max angular speed
$\theta_{\max}$	$\pi - 0.05$	Max distance
$\beta_{\max}$	10	Max convergence rate
$N_{\max}$	100	Max bisection iterations
$\omega_0$	$10[1, 1, 1]^T$	Initial angular velocity

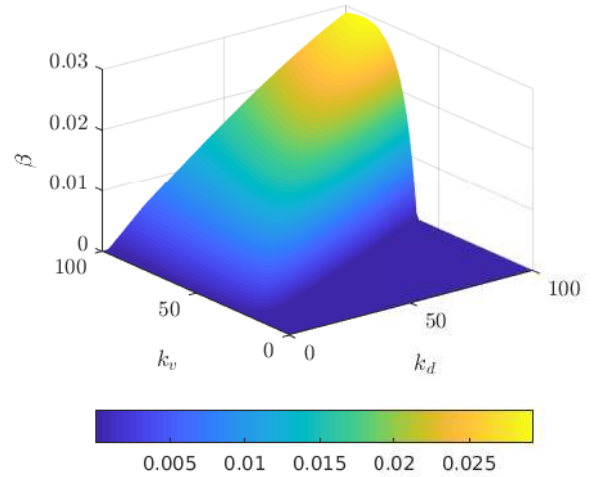


Fig. 1: A surface plot showing the optimal  $\beta$  for each pair of gains  $k_d, k_v$ . For a fixed  $k_d$ , a minimum  $k_v$  is required to find a nonzero  $\beta$ .

We can verify exponential convergence by analyzing the contraction matrix  $\mathcal{M}$ . The largest eigenvalue of the matrix  $\mathcal{M}$  using contraction parameters found in Table II is shown in Fig. 2c. As expected, the largest eigenvalue is always nonpositive thus confirming the exponential convergence by contraction theory. The simulation results suggest that we may be able to find tighter bounds on the actual limiting  $\|\omega\|_{\max}$  by reanalyzing the  $\Omega_D$  matrix using the parameters found by Algorithm 1 (this will be explored in future work).

In addition, notice that the largest eigenvalue occurs at the beginning of the trajectory where the rotation and velocity errors are maximum, implying that we can obtain tighter bounds on the minimum convergence rate  $\beta$  with smaller  $\theta_{\max}$  and  $\|\omega\|_{\max}$ . This is confirmed in Table III, last column, where the minimum convergence rate  $\beta$  increases as we restrict the system closer to the identity. In addition, one can potentially obtain better convergence rates (Table III, fourth column), by performing gain scheduling with respect to the distance to the equilibrium, and using optimal gains for each region (Table III, second and third columns).

#### V. CONCLUSION

We have shown that a simple geometric PD controller can have a large exponential convergence region, and we proposed a way to automatically choose controller gains based on a lower bound of the system's exponential convergence rate. The

TABLE II: Algorithm 1 Results

Parameter	Value	Description
$\beta$	0.0292	Fastest convergence rate
$k_d$	100	Rotation error gain
$k_v$	89.9091	Angular velocity error gain
$m_1$	1.0000	Metric $\tilde{g}$ gain
$m_2$	0.0110	Metric $\tilde{g}$ gain
$m_3$	0.0003	Metric $\tilde{g}$ gain

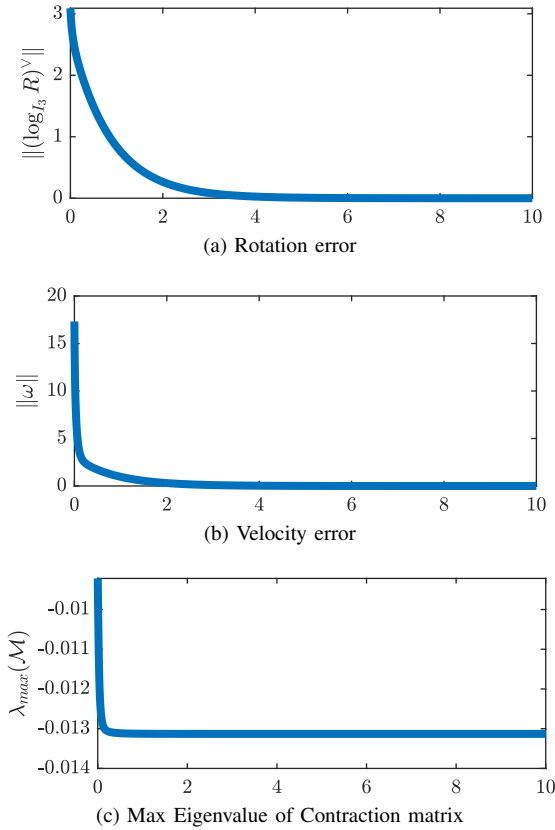


Fig. 2: Simulation results using parameters from Table II. The maximum eigenvalue of the contraction metric in 2c is always nonpositive, therefore the system is exponentially converging.

TABLE III: Convergence Rate and Max Distance

$\theta_{max}$	$k_d^*$	$k_v^*$	$\beta^*$	$\beta(k_v = 89.9091)$
$\pi - 0.05$	100	89.9091	0.0292	0.0292
$3\pi/4$	100	38.4455	1.0453	0.5372
$\pi/2$	100	26.3364	2.5162	0.8775
$\pi/4$	100	21.2909	4.0287	1.0648

underlying concept is the idea of contraction on manifolds, and the fact that the contraction metric can be formulated as a linear matrix inequality. We showed that for rigid body three-dimensional rotations, the contraction metric has a particular form that can be exploited to give linear optimization objectives and constraints. We also showed that for a particular choice of cost function, we can find a quasi-global exponentially stable geometric attitude controller.

In future work, we plan to investigate other potential functions  $\Psi$ , and to apply our framework to the manifold of three-dimensional rigid poses  $SE(3)$ .

## REFERENCES

- [1] R. Mahony, V. Kumar, and P. Corke, “Multirotor Aerial Vehicles: Modeling, Estimation, and Control of Quadrotor,” *IEEE Robotics and Automation Magazine*, vol. 19, no. 3, pp. 20–32, 2012.
- [2] M. D. Shuster, “A Survey of Attitude Representations,” *Journal of the Astronautical Sciences*, vol. 41, pp. 439–517, Oct. 1993.
- [3] J.-Y. Wen and K. Kreutz-Delgado, “The attitude control problem,” *IEEE Transactions on Automatic Control*, vol. 36, no. 10, pp. 1148–1162, 1991.
- [4] A. Tayebi and S. McGilvray, “Attitude stabilization of a vtol quadrotor aircraft,” *IEEE Transactions on Control Systems Technology*, vol. 14, no. 3, pp. 562–571, May 2006.
- [5] D. E. Koditschek, “The application of total energy as a lyapunov function for mechanical control systems,” *Contemporary Mathematics*, vol. 97, p. 131, 1989.
- [6] F. Bullo and R. M. Murray, “Tracking for fully actuated mechanical systems: a geometric framework,” *Automatica*, vol. 35, no. 1, pp. 17–34, 1999.
- [7] D. S. Maithripala, J. M. Berg, and W. P. Dayawansa, “Almost-global tracking of simple mechanical systems on a general class of lie groups,” *IEEE Transactions on Automatic Control*, vol. 51, no. 2, pp. 216–225, 2006.
- [8] T. Lee, M. Leok, and N. McClamroch, “Control of complex maneuvers for a quadrotor UAV using geometric methods on  $SE(3)$ ,” *arXiv preprint arXiv:1003.2005*, no. 3, pp. 1–32, 2010.
- [9] N. A. Chaturvedi, A. K. Sanyal, and N. H. McClamroch, “Rigid-body attitude control,” *IEEE Control Systems Magazine*, vol. 31, no. 3, pp. 30–51, 2011.
- [10] K. Sreenath, T. Lee, and V. Kumar, “Geometric control and differential flatness of a quadrotor UAV with a cable-suspended load,” *IEEE International Conference on Decision and Control*, vol. 1243000, pp. 2269–2274, 2013.
- [11] S. Berkane, A. Abdessameud, and A. Tayebi, “Hybrid global exponential stabilization on  $SO(3)$ ,” *Automatica*, vol. 81, pp. 279–285, 2017.
- [12] C. G. Mayhew and A. R. Teel, “Hybrid control of rigid-body attitude with synergistic potential functions,” in *IEEE American Control Conference*, 2011, pp. 287–292.
- [13] ———, “Synergistic potential functions for hybrid control of rigid-body attitude,” in *IEEE American Control Conference*, 2011, pp. 875–880.
- [14] T. Lee, “Global exponential attitude tracking controls on  $SO(3)$ ,” *IEEE Transactions on Automatic Control*, vol. 60, no. 10, pp. 2837–2842, 2015.
- [15] I. R. Manchester and J. E. Slotine, “Output-feedback control of nonlinear systems using control contraction metrics and convex optimization,” in *Australian Control Conference*, Nov 2014, pp. 215–220.
- [16] F. Bullo and A. D. Lewis, *Geometric control of mechanical systems : modeling, analysis, and design for simple mechanical control systems*, ser. Texts in applied mathematics ; 49. New York: Springer, 2005.
- [17] W. Lohmiller and J. Slotine, “On contraction analysis for non-linear systems,” *Automatica*, vol. 34, no. 6, 1998.
- [18] J. W. Simpson-Porco and F. Bullo, “Contraction theory on Riemannian manifolds,” *Systems and Control Letters*, vol. 65, no. 1, pp. 74–80, 2014.
- [19] J. C. H. Lee and P. Valiant, “Optimizing star-convex functions,” in *IEEE Symposium on Foundations of Computer Science*, Oct 2016, pp. 603–614.
- [20] A. Edelman, T. A. Arias, and S. T. Smith, “The Geometry of Algorithms with Orthogonality Constraints,” *SIAM Journal on Matrix Analysis and Applications*, vol. 20, no. 2, pp. 303–353, 1998.
- [21] S. Sasaki, “On the differential geometry of tangent bundles of Riemannian manifolds,” *Tohoku Mathematical Journal*, vol. 10, no. 3, pp. 338–354, 1958.
- [22] O. Kowalski, “Curvature of the Induced Riemannian Metric on the Tangent Bundle of a Riemannian Manifold,” *Journal fur die reine und angewandte Mathematik*, vol. 250, pp. 124–129, 1971.
- [23] B. Vang and R. Tron, “Non-Natural Metrics on the Tangent Bundle,” *arXiv e-prints*, p. arXiv:1809.06895, Sep 2018.
- [24] G. Strang, *Introduction to Linear Algebra*. Wellesley-Cambridge Press, 2016.
- [25] A. Gilányi, Ed., *An Introduction to the Theory of Functional Equations and Inequalities: Cauchy's Equation and Jensen's Inequality*. Basel: Birkhäuser Basel, 2009, pp. 455–481.
- [26] R. Tron, “Distributed optimization on manifolds for consensus algorithms and camera network localization,” Ph.D. dissertation, John Hopkins University, 2012.
- [27] S. P. Bhat and D. S. Bernstein, “A topological obstruction to continuous global stabilization of rotational motion and the unwinding phenomenon,” *Systems and Control Letters*, vol. 39, no. 1, pp. 63 – 70, 2000.
- [28] M. Grant and S. Boyd, “CVX: Matlab software for disciplined convex programming, version 2.1,” <http://cvxr.com/cvx>, Mar. 2014.